

## Supporting Information

### Recruitment of Receptors at Supported Lipid Bilayers Promoted by the Multivalent Binding of Ligand-Modified Unilamellar Vesicles

*Daniele Di Iorio<sup>†</sup>, Yao Lu<sup>†</sup>, Joris Meulman and Jurriaan Huskens\**

*Molecular Nanofabrication Group, MESA+ Institute for Nanotechnology, Department of Science and Technology, University of Twente, P.O. Box 217, 7500 AE, Enschede, The Netherlands*

#### Materials

Chemicals were purchased from Sigma Aldrich. 1,2-Dioleoyl-sn-glycero-3-phosphocholine (DOPC), 1,2-dioleoyl-sn-glycero-3-phosphoethanolamine-N-(cap biotinyl), sodium salt (DOPE-biotin) were purchased from Avanti Polar Lipids, while Texas Red-1,2-dihexadecanoyl-sn-glycero-3-phosphoethanolamine (TR-DHPE) was obtained from Thermo Fisher Scientific. Streptavidin and streptavidin-Alexa-Fluor<sup>®</sup> were obtained from Thermo Fischer Scientific. SAV was dissolved in 0.1 M PBS (0.01 M sodium dihydrogen phosphate and 0.15 M sodium chloride, pH 7.4) at a concentration of 20  $\mu\text{g mL}^{-1}$ .

#### Substrate cleaning and preparation

QCM-D sensors were immersed in a 2 wt% sodium dodecyl sulfate (SDS) solution for 30 min, thoroughly rinsed with Milli-Q water and dried under a nitrogen stream. Activation was performed with 20 min UV/ozone treatment using a Bioforce chamber (Nanosciences).

#### Preparation of small unilamellar vesicles (SUVs)

Lipids were first dissolved in chloroform and mixed in the desired molar ratio in a glass vial. Afterwards, the solvent was evaporated with a nitrogen stream, and the obtained lipidic film was dried for at least 1 h in a desiccator connected to a vacuum pump. The dried film was then resuspended in MilliQ water (for the formation of SUVs to form the SLBs) or PBS buffer (for the binding of SUVs onto SAV-modified SLBs) with a concentration of 1 mg/mL. The lipid suspensions were extruded 11 times through a polycarbonate membrane (Whatman) with 100 nm pore size, and the obtained SUVs were stored in the fridge and used within maximally two weeks. The size of the vesicles was measured by dynamic light scattering (DLS) before use.

#### Preparation of giant unilamellar vesicles (GUVs)

Lipids were first dissolved in chloroform and mixed in the desired molar ratio in a glass vial. Drops of the solution containing the lipid mixture were put on 2 titanium oxide-coated glass slides and

the solvent was evaporated with a flow of nitrogen gas to create uniform lipid films. The lipid-coated slides were dried in a vacuum desiccator for 1 h. The dried lipid-coated slides and a clean PDMS spacer are put together to form a capacitor cell. The conductive sides of both slides were faced inward and were fixed with a clamp to form a chamber. The chamber was filled with 200 mM sucrose buffer solution and sealed with plastic paraffin film. Electro-formation was then carried out using a function generator. A 10 Hz sinusoidal potential with a 1 V peak-to-peak amplitude was applied across the chamber for 2 h, after which the frequency was reduced to 2 Hz for 1 h. The GUVs were extracted from the chamber using a pipette, stored in an Eppendorf vial (2 mL) in the dark and used the same day. The direct usage of the GUVs is necessary because of the relatively high instability of larger vesicles.

### **Preparation of the supported lipid bilayers (SLBs) in QCM measurements**

For the fabrication of SLBs, vesicles (SUVs) were diluted to a concentration of 0.1 mg/ml in PBS buffer directly before use. SLBs were obtained by flowing this solution on a cleaned and activated SiO<sub>2</sub> surface, after obtaining a stable baseline. The quality of the SLBs was monitored by fluorescence recovery after photobleaching (FRAP, see below) or in situ by QCM-D (where high quality SLBs are defined by  $\Delta f = -24 \pm 1$  Hz and  $\Delta D < 0.5 \times 10^{-6}$ ).

### **Preparation of the supported lipid bilayers (SLBs) in FRAP and confocal microscopy measurements**

For the FRAP and GUV assembly experiments, lipid mixtures of DOPC, Texas Red-DHPE and Biotinyl-cap-PE (molar ratio 99.85:0.05:0.1) were used to form the supported lipid bilayers (SLBs) using the vesicle fusion method. SLBs were deposited in the wells of a 96-well plate with a glass bottom. Before the formation of the SLB, 400  $\mu$ L aqueous 2M sodium hydroxide solution was added to the glass substrate for 1 h to form a hydrophilic surface. Afterwards, the wells were rinsed with Milli-Q water three times and incubated with 200  $\mu$ L SUV solution for 30 min at room temperature. A defect-free SLB was then formed by the rupture of SUVs onto the hydrophilic glass substrate. Excess lipids were removed from the well by rinsing with MilliQ water three times. After SLB formation, care was taken to keep the surface submerged in buffer and without bubbles.

### **Immobilization of giant unilamellar vesicles**

Before the adhesion of GUVs, the SLB-coated substrate was incubated with Alexa Fluor 488-SAV (200  $\mu$ L, 20  $\mu$ g mL<sup>-1</sup>) for 20 min and then rinsed consecutively with PBS and sucrose buffer, each for three times. After that, 50  $\mu$ L GUV solutions were added to the well and incubated for another 30 min. Then, the well was gently rinsed with sucrose buffer three times to remove excess GUVs.

### QCM-D measurements

QCM-D measurements were performed with a Qsense Analyser from Biolin Scientific and SiO<sub>2</sub>-coated sensors (QSX303, Biolin Scientific) were used throughout this work. Measurements were done at 22 °C and operated with four parallel flow chambers, using two Ismatec peristaltic pumps with a flow rate of 20 µl/min. For every measurement, the fifth overtone was used for the normalized frequency ( $\Delta f_5$ ) and dissipation ( $\Delta D_5$ ).

In a typical experiment, SLBs were formed on previously cleaned and activated SiO<sub>2</sub> sensors. Afterwards, solutions of SAV (1 µM), of biotinylated SUVs (0.1 mg/mL) and again of SAV (1 µM) were added until a stable plateau was reached. Each step was followed by rinsing with PBS buffer. Due to the long residence time of the SAV-biotin interaction, it is reasonable to exclude any competitive binding of free additional SAV with already bound biotins.

In order to estimate whether or not differences in biotin density in the SUVs and SLBs affect the way in which the vesicles are adsorbed on the surface, *e.g.*, by affecting the contact area and/or the viscoelastic properties of the vesicle-SLB layer, the ratio between  $\Delta D_5$  and  $\Delta f_5$  was determined for each SUV step (Figure 2C). Interesting changes in the ratio were observed, indicating changes in viscoelastic properties as a function of biotin densities in SLB and SUVs. The  $\Delta D_5/\Delta f_5$  ratios were measured for each set of experiments using 0.1%, 0.4% and 2.0% of biotin molar fraction in the SLB. Interestingly, differences were observed between these series of measurements, obtained for different SAV densities on the SLB. Specifically, a lower  $\Delta D_5/\Delta f_5$  ratio was observed for vesicles adsorbed on SLBs containing a higher SAV density, particularly evident again at high biotin% in the SUVs. Therefore a high SAV density on the surface appeared to lead to an increased stiffness of the surface upon binding of vesicles with clear differences between SUVs containing high biotin contents. At very low percentages of biotin in the SUVs, instead, similar  $\Delta D_5/\Delta f_5$  ratios were observed, despite the differences in SAV density on the surface.

### FRAP measurements

By a confocal microscope, a circular spot of 10 µm in diameter was bleached, then the fluorescence intensity in the bleached regions was monitored. For the SLB immobilized at the bottom of the 96-well plate, the FRAP protocol consisted of 11 imaging loops (1 s interval) before bleaching, 10 loops bleaching with no delay in between loops, and 300 loops of recovery (1 s interval). Then the FRAP curves were fitted in a diffusion model for circular spot by the modified Bessel functions.<sup>1</sup>

### Confocal microscopy

Confocal laser scanning microscopy (CLSM, Nikon A1) was used to observe immobilized GUVs and the SLB. The Texas Red-labeled GUVs were examined by CLSM at an excitation wavelength ( $\lambda_{ex}$ ) of 595 nm, while the Alexa Fluor 488 SAV was measured at  $\lambda_{ex}$  of 495 nm.

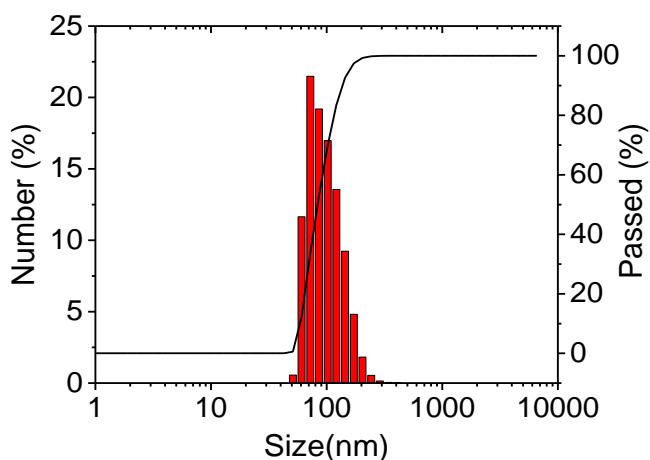


**Figure S1.** DLS of SUVs containing 1% of DOPE-biotin for the formation of lipid bilayers

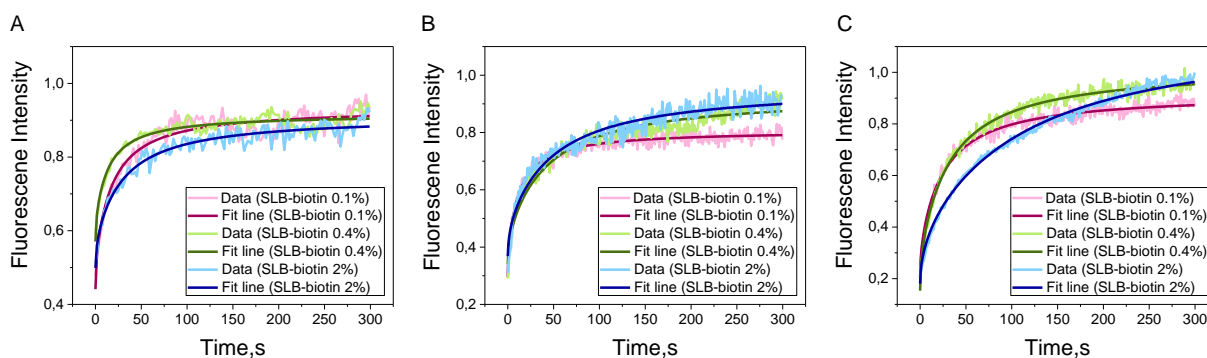


**Figure S2.** Confocal FRAP curves on SLBs with 0.1, 0.4 and 2 mol% biotin. FRAP of the Texas Red-labeled SLB (A) before and (B) after the anchoring of Alexa Fluor 488-labeled SAV. (C) FRAP curves of the Alexa Fluor 488-labeled SAV anchored on the SLB. The fitted curves were obtained from the modified Bessel function and the fitted diffusion constants are listed in Table S2. The FRAP curves were fitted to a diffusion model modified by the Bessel function<sup>1</sup> from which the diffusion coefficients of the lipids for each SLB composition were obtained (see Table S1).

**Table S1.** Diffusion coefficients determined with the FrapAnalyser from Luxembourg University.<sup>1</sup> Processed with double normalization and a modified Bessel fitting.

DOPE-biotin in SLB (mol%)	Diffusion constant of SLB before SAv ( $\mu\text{m}^2/\text{s}$ )	Diffusion constant of SLB after SAv ( $\mu\text{m}^2/\text{s}$ )	Diffusion constant of SAv ( $\mu\text{m}^2/\text{s}$ )
0.1	$1.7 \pm 0.3$	$2.5 \pm 0.2$	$1.2 \pm 0.1$
0.4	$1.2 \pm 0.4$	$0.76 \pm 0.10$	$0.97 \pm 0.06$
2	$1.1 \pm 0.2$	$0.68 \pm 0.09$	$0.31 \pm 0.02$

**Table S2.** Size of SUVs containing varying molar fractions of DOPE-biotin determined by DLS.

DOPE-biotin in DOPC vesicles (%)	Vesicles size (nm)
0.025	$90 \pm 30$
0.1	$86 \pm 29$
0.25	$92 \pm 30$
0.4	$83 \pm 27$
0.6	$92 \pm 28$
1.0	$93 \pm 30$
5	$79 \pm 26$

Differences in size between SUVs with different biotin fractions measured with DLS were within 10%. Moreover, no correlation was observed between vesicle size and the biotin content, therefore the small differences can be attributed exclusively to variations in preparation. Other factors, such as different molecular weights due to the presence of different DOPE-biotin molar ratios, were found negligible considering the low fractions used.

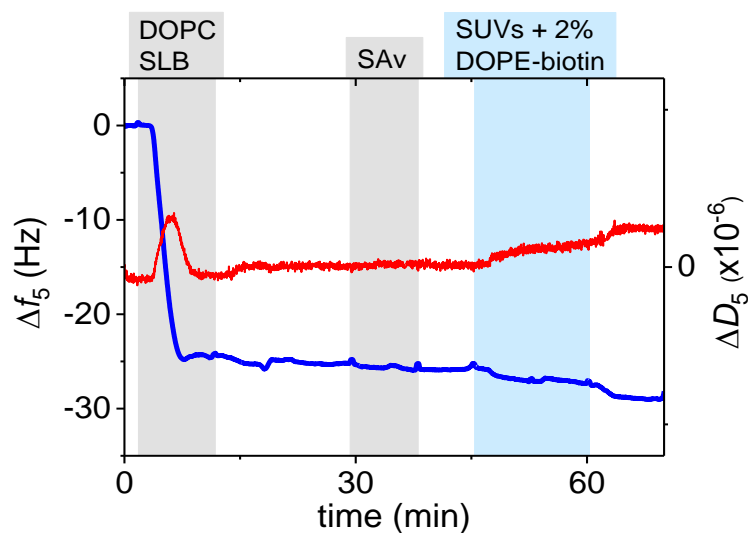


**Figure S3.** QCM-D measurement representing the formation of a DOPC SLB (without DOPE-biotin) followed by the addition of SAv and SUVs containing 2% of DOPE-biotin. The different shadings correspond to the different additions. White areas correspond to PBS washing steps.

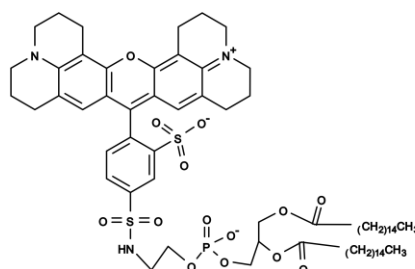


**Figure S4.** Chemical structure of Texas Red-DHPE.

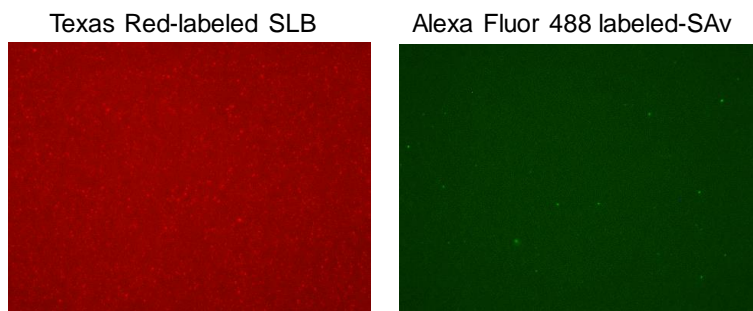


**Figure S5.** Texas Red-labeled SLB (from 0.05 mol% Texas Red-DHPE in DOPC, with 0.1 mol% biotin-DOPE) functionalized with Alexa Fluor 488-SAv before the binding of GUVs.

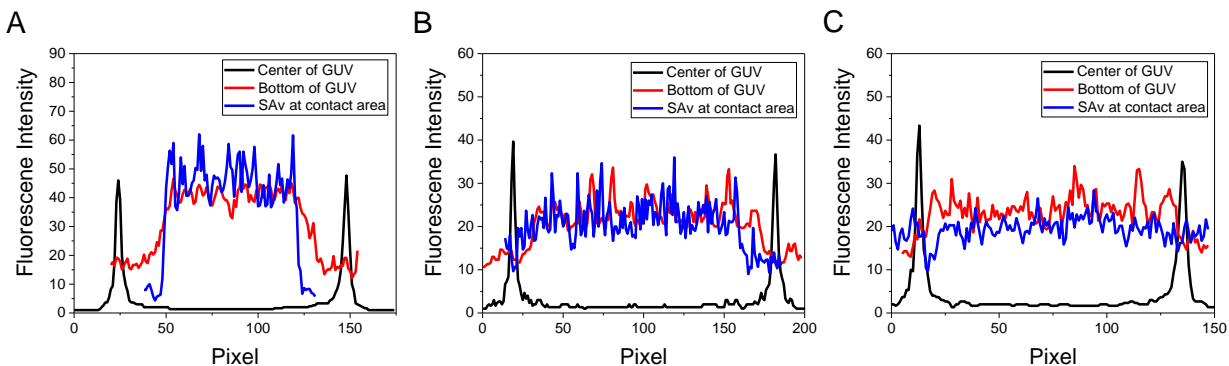


**Figure S6.** The fluorescence profiles of immobilized GUVs on the SLB. (A) 0.1 mol% biotin-GUV on 0.1 mol% biotin-SLB, (B) 0.1 mol% biotin-GUV on 0.4 mol% biotin-SLB, (C) 0.1 mol% biotin-GUV on 2 mol% biotin-SLB.

### Quantitative analysis of the deformation of GUVs

To quantitatively analyze the deformation of GUVs after receptor clustering, changes of the area ratio of a GUV, which was defined as the ratio between the contact area (3<sup>rd</sup> column in Figure 3) and the projected (widest/center) area of a GUV (1<sup>st</sup> column in Figure 3), were plotted as a function of the vesicle size (Figure S7A). The morphological changes depended on the fraction of biotin receptors at the SLB interface, as shown in Figure S8A. In the case of 0.1 mol% biotin, the area ratio almost stayed constant at around 0.25 independent of the vesicle size, however, this value reached approx. 0.8 when the biotin density in the SLB was raised to 0.4 or 2 mol%, indicating that a larger deformation of vesicles was induced by higher receptor densities.

Furthermore, the receptor clustering was studied by changing the biotin density in the GUVs (0.1, 0.4 and 2 mol%) adsorbing onto SLBs with a fixed biotin concentration (0.1 mol%). As Figure S9A shows, the green fluorescence of the contact areas for GUVs with 0.4 and 2 mol% biotin was all bright and with high contrast, comparable to the GUVs with 0.1 mol% biotin (1st row in Figure 3), indicating an efficient clustering of SAv molecules on the SLB at a low receptor density (0.1 mol% biotin) regardless of the biotin density in the vesicles. Although the fluorescence intensities of SAv at the contact area for GUVs with different biotin densities were not that different (Figure S9B and S9C), the area ratios in these three cases were distinct from each other.

By extracting the area ratios of vesicles of different sizes (Figure S7B), the morphological changes for GUVs of different biotin densities are shown in Figure S8B. Similar to the trend in Figure S8A, the area ratios of vesicles increased also when the biotin densities in the GUVs were increased to 0.4 and 2 mol%. This suggests that, in the case of 0.1 mol% biotin in the GUVs, all biotin moieties from the GUVs can be arranged into biotin-SAv interaction pairs within a relatively small area. When the biotin density in the GUVs is increased to 0.4 and 2 mol%, more biotin-SAv interaction pairs are formed, which induces larger morphological changes.

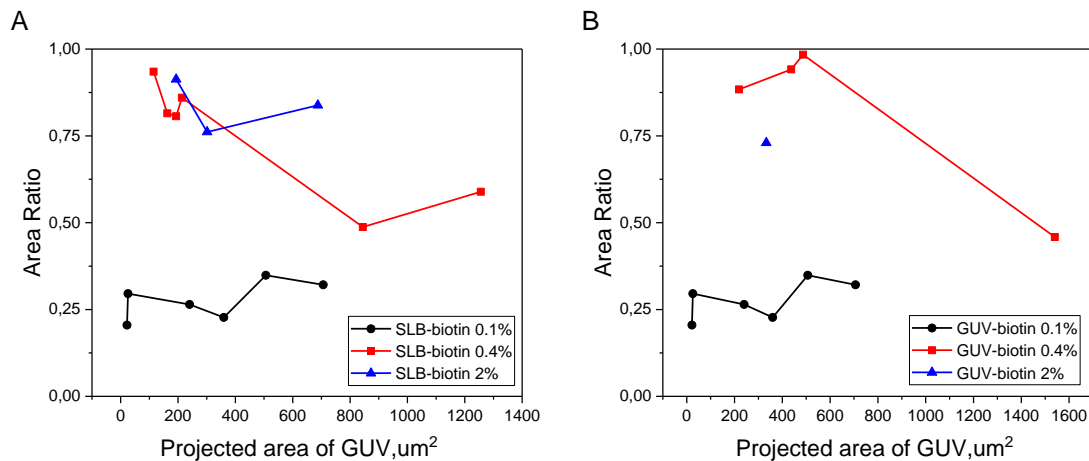


**Figure S7.** Changes of area ratios as a function of the GUVs projected area (i.e. the cross-section area). (A) GUVs with 0.1 mol% biotin immobilized on the SLB of different biotin densities (0.1, 0.4 and 2 mol%). (B) GUVs with different biotin densities (0.1, 0.4 and 2 mol%) immobilized on the SLB with 0.1 mol% biotin.

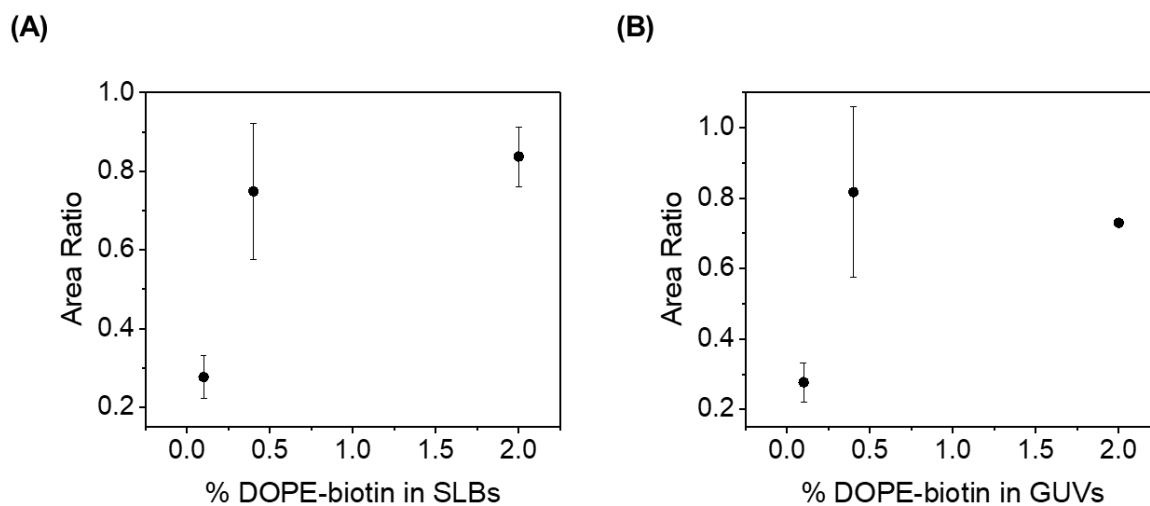


**Figure S8.** (A) Area ratios of the contact area (3rd column in Figure 3) and the cross-section area (1st column in Figure 3) of GUVs (with 0.1 mol% biotin) immobilized on SLBs with different biotin densities (0.1, 0.4 and 2 mol%). (B) Area ratios of GUVs containing different biotin densities (0.1, 0.4 and 2 mol%) immobilized on SLBs with 0.1 mol% biotin. Here only one datapoint is shown for 2 mol% DOPE-biotin in the GUVs due to a lower vesicle stability in this case. Area ratios as a function of GUV size are shown in Figure S7.

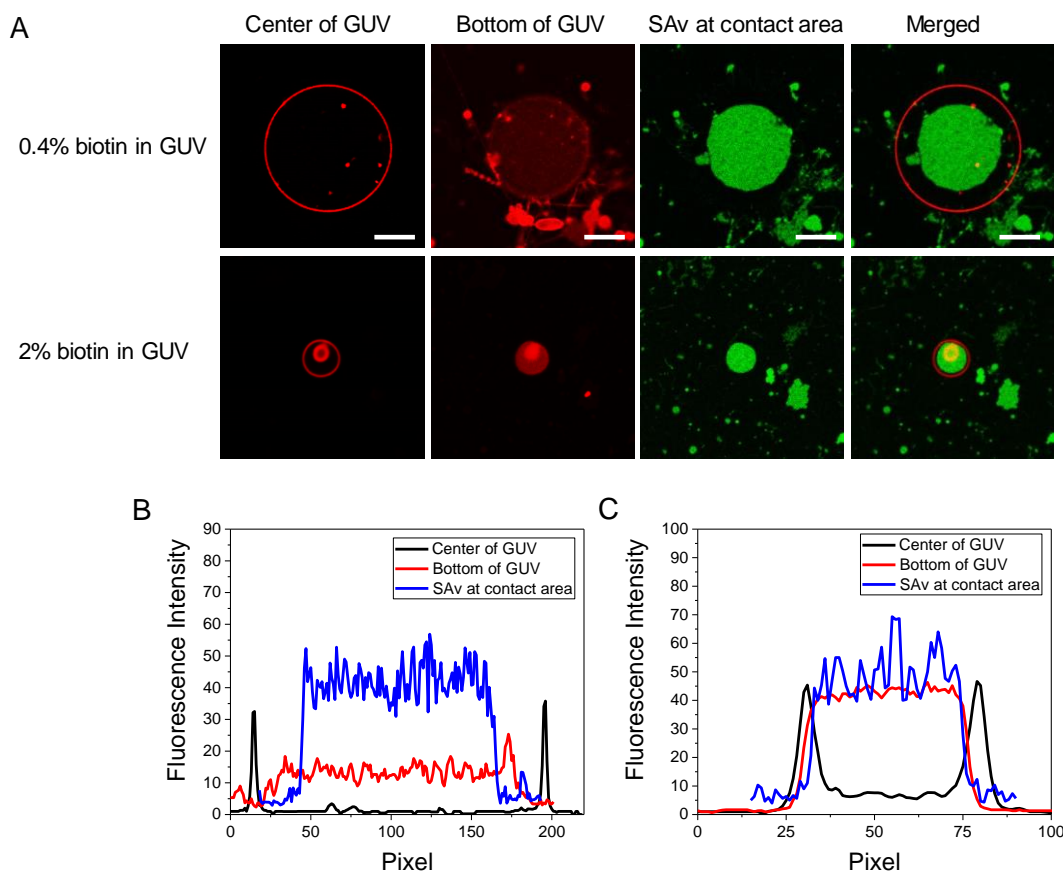


**Figure S9.** (A) Fluorescence microscopy images of the immobilized GUVs with biotin ligands of different densities (0.4 and 2 mol%) on SLBs with 0.1% biotin. 1<sup>st</sup> column: the widest/center section of the GUV; 2<sup>nd</sup> column: the bottom of GUVs obtained from the contact area between the GUV and the SLB; 3<sup>rd</sup> column: clustering of SA<sub>v</sub> molecules at the contact area; 4<sup>th</sup> column: merged images of the 1<sup>st</sup> and 3<sup>rd</sup> columns. Scale bars indicate 5 μm. (B) The fluorescence intensity profiles of GUVs with 0.4 mol% biotin immobilized on the SLB with 0.1 mol% biotin. (C) The fluorescence intensity profiles of GUVs with 2 mol% biotin immobilized on the SLB with 0.1% biotin.

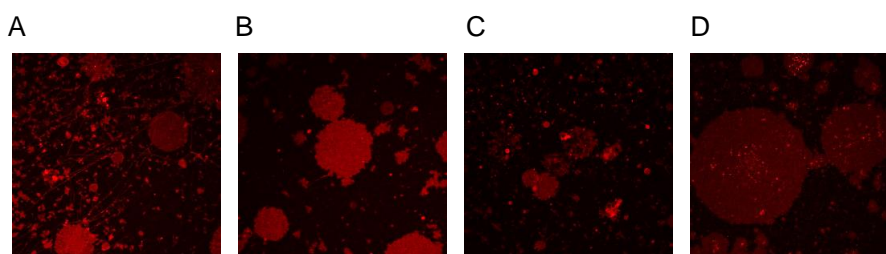


**Figure S10.** Ruptured GUVs on the SLB. (A) 0.4 mol% biotin-GUV on 0.4 mol% biotin-SLB, (B) 0.4 mol% biotin-GUV on 2 mol% biotin-SLB, (C) 2 mol% biotin-GUV on 0.4 mol% biotin-SLB, (D) 2 mol% biotin-GUV on 2 mol% biotin-SLB.

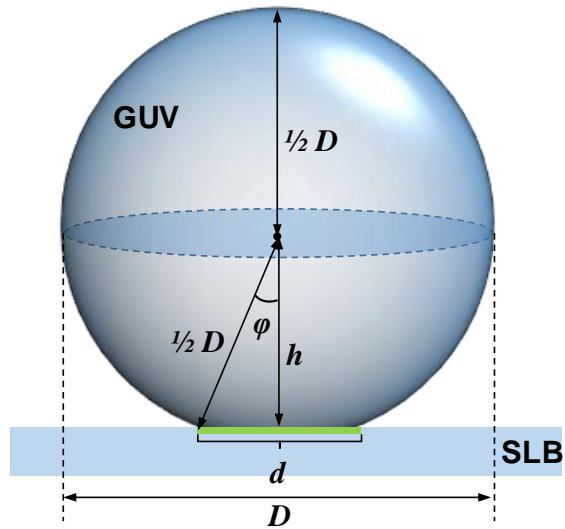


**Figure S11.** Calculation model of the capped-sphere for immobilized GUV on the SLB.

### Calculation of the quantification of streptavidin (SAv) on a surface

Assuming that one DOPC lipid covers  $0.725 \text{ nm}^2$ , *i.e.* a lipid density in the SLB corresponding to  $1.38 \text{ molecule per nm}^2$  ( $= 2.3 \times 10^{-10} \text{ mol/cm}^2 = a$ ), and that a SAv binds to two biotin in SLB, we obtain as follows:

- fraction DOPE-biotin =  $x$ ;
- density of DOPE-biotin =  $x \times a = xa$ ;
- density of SAv =  $\frac{1}{2}xa$ ;

Therefore at  $x = 0.1\%$ : Density of SAv =  $0.11 \text{ pmol/cm}^2$ , *etc.*

### Calculations of SAv numbers in Table S3 by using the parameters labeled in Figure S10

- the surface area of the capped GUV:  $A_{cap} = \pi * D * (h + d/2)$
- the contact area of a GUV:  $c.a. = \pi * (d/2)^2$
- the surface area of an intact GUV:  $A_{ves} = A_{cap} + c.a.$
- the equivalent diameter of the capped GUV:  $D' = \text{sqrt}(A_{ves}/\pi)$
- the area ratio of the contact area to the project area of a GUV:  $\text{area ratio} = d^2/D^2$
- the number of lipids in a GUV:  $\# lip ves = (A_{ves} * 10^6)/25$
- the number of biotinyl lipids in a GUV (with 0.1 mol% biotin):  $\# biotin ves = \# lip ves * 0.1\%$
- the area of the recruited SAv:  $c.a. recr SAv = \frac{1}{2} \# biotin ves * 25 * 10^{-6}$
- the ratio of the contact area to the area of the recruited SAv:  $c.a. ratio = c.a./c.a. recr SAv$

**Table S3.** Comparison between the experimental and the maximum theoretical number of SAV in binding sites for the GUVs with 0.1 mol% biotin that are immobilized on the SLB of 0.1 mol% biotin (parameters are labelled in Figure S10).

% biotin in SLB	D ( $\mu\text{m}$ )	d ( $\mu\text{m}$ )	d/D	$\sin(\varphi)$	arcsine ( $\varphi$ )	h ( $\mu\text{m}$ )	A cap ( $\mu\text{m}^2$ )	c.a. ( $\mu\text{m}^2$ )	A ves ( $\mu\text{m}^2$ )	D' ( $\mu\text{m}^2$ )	Area ratio	c.a. /A ves	# lip ves	% biotin in GUV	#biotin ves	c.a. recrSav ( $\mu\text{m}^2$ )	c.a. ratio
0,1	30	17	0,57	0,60	12,36	2578,55	226,98	2805,53	29,88	0,32	0,08	3,87E+09	0,1	3,87E+06	48,37	4,69	
0,1	25,4	15	0,59	0,63	10,24	1831,24	176,71	2007,96	25,28	0,35	0,09	2,77E+09	0,1	2,77E+06	34,62	5,10	
0,1	21,4	10,2	0,48	0,50	9,41	1351,75	81,71	1433,47	21,36	0,23	0,06	1,98E+09	0,1	1,98E+06	24,71	3,31	
0,1	17,5	9	0,51	0,54	7,50	893,62	63,62	957,24	17,46	0,26	0,07	1,32E+09	0,1	1,32E+06	16,50	3,85	
0,1	5,7	3,1	0,54	0,58	2,39	93,86	7,55	101,41	5,68	0,30	0,07	1,40E+08	0,1	1,40E+05	1,75	4,32	
0,1	5,3	2,4	0,45	0,47	2,36	83,46	4,52	87,99	5,29	0,21	0,05	1,21E+08	0,1	1,21E+05	1,52	2,98	
0,4	40	30,7	0,77	0,87	12,82	4124,41	740,23	4864,64	39,35	0,59	0,15	6,71E+09	0,1	6,71E+06	83,87	8,83	
0,4	32,8	22,9	0,70	0,77	11,74	2899,80	411,87	3311,67	32,47	0,49	0,12	4,57E+09	0,1	4,57E+06	57,10	7,21	
0,4	16,5	15,3	0,93	1,19	3,09	587,75	183,85	771,61	15,67	0,86	0,24	1,06E+09	0,1	1,06E+06	13,30	13,82	
0,4	15,7	14,1	0,90	1,12	3,45	557,48	156,15	713,62	15,07	0,81	0,22	9,84E+08	0,1	9,84E+05	12,30	12,69	
0,4	14,4	13	0,90	1,13	3,10	465,82	132,73	598,55	13,80	0,82	0,22	8,26E+08	0,1	8,26E+05	10,32	12,86	
0,4	12,1	11,7	0,97	1,31	1,54	288,62	107,51	396,14	11,23	0,93	0,27	5,46E+08	0,1	5,46E+05	6,83	15,74	
2	29,6	27,1	0,91	1,16	5,95	1929,84	576,80	2506,64	28,25	0,84	0,23	3,46E+09	0,1	3,46E+06	43,22	13,35	
2	19,6	17,1	0,87	1,06	4,79	898,34	229,66	1128,00	18,95	0,76	0,20	1,56E+09	0,1	1,56E+06	19,45	11,81	
2	15,7	15	0,96	1,27	2,32	501,51	176,71	678,22	14,69	0,91	0,26	9,35E+08	0,1	9,35E+05	11,69	15,11	

## References

1. D. M. Soumpasis, *Biophys. J.*, 1983, **41**, 95-97.